Available online at www.sciencedirect.com
SCIENCE DIRECT®
Biochemical and Biophysical Research Communications 308 (2003) 300–305
BBRC
www.elsevier.com/locate/ybbrc

The conserved P1′ Ser of Bowman–Birk-type proteinase inhibitors is not essential for the integrity of the reactive site loop

Arnd B.E. Brauer and Robin J. Leatherbarrow*

Department of Chemistry, Imperial College London, South Kensington Campus, London SW7 2AZ, UK

Received 1 July 2003

Abstract

The isolated reactive site β-hairpin loop of Bowman–Birk-type proteinase inhibitors has become a widely studied proteinomimetic because it retains the three-dimensional structure and much of the inhibitory potency of the corresponding region of the complete protein. Here we analyse the role of the P1′ Ser residue which is highly conserved and intramolecularly hydrogen bonded in the complete proteins. A combined kinetic and structural analysis of variant proteinomimetic peptides demonstrates that the hydrogen-bond potential of the side-chain oxygen atom of the P1′ Ser is not essential for the integrity of the reactive site loop and that it provides only a small contribution to the trypsin affinity and no apparent contribution to the stability against tryptic turnover. We conclude that the potential of the P1′ side chain to engineer improved inhibition and selectivity for serine proteinases is best explored further in concert with the side chains of the P2 and P5′ residues which may interact or compete for the same space.

Keywords: Proteinomimetic; β-Hairpin peptide; Type VI β turn; *cis*/*trans* Proline isomerisation; NMR spectroscopy; Sunflower trypsin inhibitor I

The reactive site loop sequence of Bowman–Birk proteinase inhibitors (BBIs [1]; also present in sunflower trypsin inhibitor 1, SFTI-1 [2]) has recently been identified as an independent structural β-hairpin motif [3]. This motif is a minimal peptide scaffold that incorporates the 'canonical' backbone conformation typically found in small serine protease inhibitor proteins [4]. This motif has attracted much interest as a proteinomimetic peptide (reviewed in [5]) because it can retain the protein-like structure and potent biological activity. In order to understand the sequence-inherent stability of this system and thereby to explore its potential for engineering biological activity, detailed structure–activity studies have been performed on several residues within its covalently closed nine-residue reactive site loop. The P1 residue (Schechter and Berger nomenclature [6]) has been shown to be the prime determinant of proteinase specificity [7]. The P2 Thr and the P2′ Ile are particularly suitable residues to achieve high levels of both affinity and resistance against proteolytic breakdown [8–10]. The strictly conserved P3′ Pro is essential for the native-like *cis* peptide bond at that position, whereas the P4′ Pro has a role supportive of the preceding P3′ *cis*-Pro [11,12]. Covalent cyclisation of the nine-residue loop is essential for potent inhibition [7], but the native disulfide bridge that tethers the P3 and P6′ positions can be replaced by an alternative linkage [12].

Here we focus on the conserved P1′ Ser residue and present the first structure–activity study that combines detailed kinetic and NMR analyses. A classic review of protein inhibitors of proteinases emphasised the unusual "stubborn conservation of P1′ Ser in all known Bowman–Birk inhibitors" [13]. This finding, with only single exceptions, has been confirmed by a more recent review [14]. X-ray crystal structures of BBI proteins [15–20] and SFTI-1 [2] consistently indicate that the P1′ Ser side chain participates in an intramolecular hydrogen-bond network within the reactive site loop. We therefore chose to analyse in detail the functional and structural effects of selectively disabling the potential for side-chain hydrogen bonding by a P1′ Ser → Ala substitution in the anti-tryptic loop. As this substitution was found to affect

* Corresponding author. Fax: +44-207-594-5880.
E-mail address: R.Leatherbarrow@imperial.ac.uk (R.J. Leatherbarrow).

0006-291X/$ - see front matter © 2003 Elsevier Inc. All rights reserved.
doi:10.1016/S0006-291X(03)01365-2

in particular the NOE pattern of the P5′ Gln side chain, the analysis was extended to the corresponding P5′ Gln → Ala variant in order to test for an intramolecular communication.

Materials and methods

The employed materials and methods have been described in detail for the previous analysis of the strictly conserved P3′ Pro residue in the same model system [11]. In short, the peptides were synthesised by using the Fmoc strategy with HBTU/HOBt activation and disulfide-cyclised in solution by oxidisation with dimethyl sulfoxide. The chemical homogeneity and the identity of the peptides were confirmed by analytical reversed-phase HPLC and fast atom bombardment mass spectrometry, respectively. For enzyme assays, the concentration of bovine pancreatic trypsin was determined by active site titration with *p*-nitrophenyl *p*′-guanidino benzoate. Trypsin inhibition was monitored by competitive binding studies with the chromogenic substrate benzoyl-L-arginine *p*-nitroanilide [21] in 50 mM Tris–HCl buffer containing 50 mM NaCl, 10 mM $CaCl_2$ at pH 8.0 and 298 K. Substrate concentration was determined by the final absorbance at 410 nm. Peptide concentrations were determined by measuring the absorbance at 280 nm [22]. The non-linear regression software package GraFit (Erithacus Software) was used to analyse the inhibition data assuming the tight-binding inhibition equation:

$$v = v_0 \cdot \left\{ [E_0] - \left((K_{d*} + [E_0] + x \cdot [I_0]) - \sqrt{(K_{d*} + [E_0] + x \cdot [I_0])^2 - 4 \cdot [E_0] \cdot x \cdot [I_0]} \right) \right\} \Big/ \{2 \cdot [E_0]\}.$$

The rate of enzymatic substrate hydrolysis v is expressed as a function of the uninhibited rate v_0, the apparent equilibrium dissociation constant K_{d*}, total enzyme concentration $[E_0]$, and total inhibitor concentration $[I_0]$. A factor x for the inhibitor concentration was introduced to determine the apparent binding stoichiometry. This is interpreted as the inhibitory active fraction of peptide which decreases with incubation time as a result of enzymatic turnover. The equilibrium dissociation constant K_d was calculated by correction for substrate competition, with $[S_0]$ and K_M being the total substrate concentration and Michaelis constant, respectively:

$$K_d = K_{d*} \cdot \frac{1}{1 + \frac{[S_0]}{K_M}}.$$

The ^1H NMR analysis was performed in aqueous solution (90% H_2O/10% ^2H_2O and 100% ^2H_2O; with and without 50 mM phosphate buffer) at a pH* of 3.8 and temperatures between 275 and 305 K by using standard DQF-COSY, TOCSY (mixing time 80 ms), NOESY (mixing times of 100, 200, and 300 ms), and ROESY (mixing time 200 ms) experiments recorded on a Bruker AMX 600 spectrometer. 3-(Trimethylsilyl)-1-propanesulfonic acid was used as an internal reference. All coupling constants were derived from one-dimensional spectra. Model building and refinement for all three peptides were performed with the software package TINKER [23] using the AMBER force field. The program DISTGEOM was used to refine model structures against the NMR-derived restraints with the distance geometry and simulated annealing protocol that has been described in detail in the original publication [23]. Interproton distance restraints were classified into three ranges: 1.86–2.50, 1.86–3.30, and 1.86–5.00 Å. ϕ-Restraints were implemented in three ranges: −150° to −90°, −75° to −55°, and −180° to −60° for residues with observed $^3J_{HNH\alpha}$ coupling constants $\geqslant 9.0$ Hz, for Pro residues, and for the remaining residues, respectively. Experimentally determined preferred χ^1 rotamers [24] were implemented with bounds of ±30°. No hydrogen-bond restraints were used in the structure calculations. All residues of the final structures fall into the favoured or additionally allowed regions of the Ramachandran plot as assessed with the program PROCHECK [25].

Results and discussion

Substitution of the conserved P1′ Ser

The effects of the P1′ Ser → Ala substitution in the isolated anti-tryptic BBI reactive site loop, here referred to as the template peptide, on the biological activity are summarised in Table 1 (see also Fig. 1. The equilibrium dissociation constant with trypsin is increased fourfold, the estimated inhibitory active fraction (x at zero time) is increased, whereas the resistance against tryptic turnover is not significantly different within experimental error. In the previous analyses of the roles of the strictly conserved P3′ Pro [11] and the highly conserved P2 Thr [9], we have demonstrated that the kinetically observed active fraction is correlated with the balance between the protein-like conformer and alternative less potent or even inactive conformers that arise from *cis*/*trans* peptide bond isomerisation. While it is difficult to relate exactly the proportions of different conformers with the apparent binding stoichiometry (the pH and the concentration conditions are necessarily different and complex formation is unlikely to be instantaneous as assumed by the model), the kinetically observed trend is supported by the NMR spectra (Fig. 2). These show that the population of the dominant conformer of the P1′ Ala variant is increased at the expense of alternative conformers compared with the template peptide. We achieved complete assignment of the dominant P1′ Ala conformer and used a combination of distance geometry

Table 1
Sequences and inhibition parameters of the disulfide-cyclised proteinomimetic peptides

Variant peptide	Sequence											K_d (nM)	x at zero time	$t_{1/2}$ (min)
	P4	P3	P2	P1	P1′	P2′	P3′	P4′	P5′	P6′	P7′			
Template	S	C	T	K	S	I	P	P	Q	C	Y	35 ± 5	0.55 ± 0.04	7.2 ± 1.8
P1′ Ala	S	C	T	K	**A**	I	P	P	Q	C	Y	139 ± 47	0.78 ± 0.05	6.8 ± 0.8
P5′ Ala	S	C	T	K	S	I	P	P	**A**	C	Y	130 ± 66	0.52 ± 0.02	6.4 ± 0.4

The equilibrium dissociation constant with bovine pancreatic trypsin (K_d), the extrapolated inhibitory active fraction of the peptide (x) at zero exposure time, and its estimated half-life time of tryptic turnover ($t_{1/2}$) were derived from plots as exemplarily shown in Fig. 1.

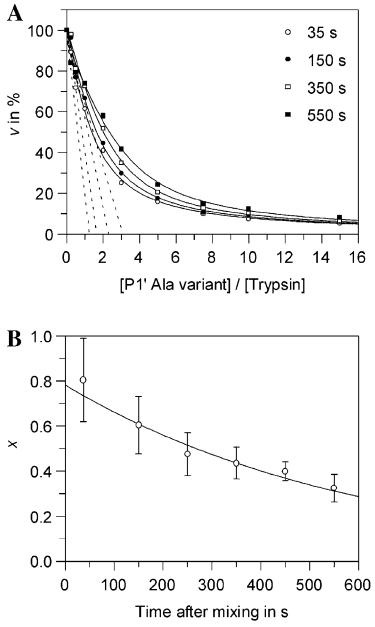

Fig. 1. (A) A family of inhibition curves at different times after mixing P1′ Ala variant peptide and bovine pancreatic trypsin (the enzyme concentration was 0.38 μM; for clarity only a subset of the experimental results is presented). The curves are best fits assuming tight-binding behaviour. The dotted lines visualise the change of apparent binding stoichiometry. (B) The inhibitory active fraction of P1′ Ala variant (x) as a function of time after mixing as derived from the inhibition curves in (A). The data are described by a single exponential curve assuming an apparent first-order process. The inhibitory active fraction of peptide in the absence of enzyme and its rate of tryptic hydrolysis were estimated from the intercept at zero time and the curvature, respectively.

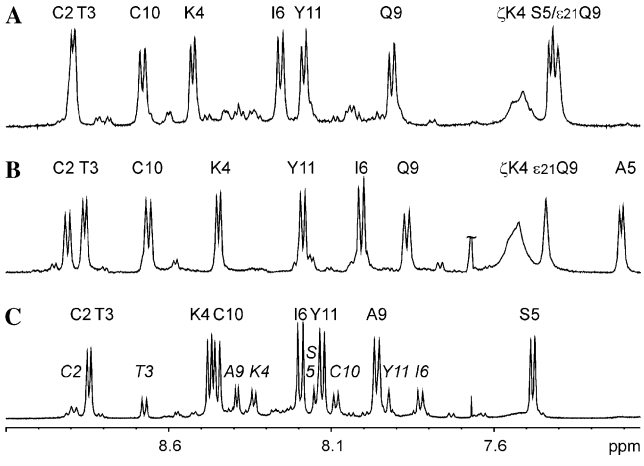

Fig. 2. Amide region of the one-dimensional 600 MHz ^{1}H NMR spectrum of the template (A), the P1′ Ala variant (B), and the P5′ Ala variant (C) in aqueous solution at pH* 3.8 and 298 K (an impurity in the solvent has been cropped (∼) for clarity). The HN resonances of fully assigned conformers are labelled.

and simulated annealing methods to calculate a family of 20 lowest-energy structures which is consistent with the combined NMR-derived restraints. These restraints consisted of NOE-derived distances (17 sequential (i, $i+1$), 3 medium range (i, $i+2$ to i, $i+4$), and 7 long range (i, $i+6$ to i, $i+8$)), and of dihedral angles (10ω, 10ϕ, $4\chi^1$) that were derived from coupling constants and/or NOE connectivities. Fig. 3 shows that the P1′ Ala variant retains the three-dimensional structure of the corresponding region of the complete BBI protein almost as well as the template peptide, an NMR-derived solution structure of which we have previously described in detail (RCSB protein database accession code 1gm2 [26]).

These findings demonstrate that the P1′ Ser → Ala substitution is well tolerated and that the conserved P1′ Ser is therefore not essential for the integrity of the BBI reactive site loop. This would not have been easy to predict from the available protein information which characterises the P1′ Ser as highly conserved and hydrogen bonded. This finding contrasts with the significant changes that are associated with substitutions of the highly conserved and hydrogen-bonded P2 Thr residue and of the strictly conserved P3′ Pro residue. The elimination of the side-chain hydrogen-bond potential of the P2 residue induced significant structural rearrangements and accelerated enzymatic turnover [9], whereas the substitution of the P3′ Pro resulted in a structural and functional breakdown [11]. It is particularly surprising that the P1′ Ser → Ala substitution enhances the population of the protein-like conformer. The NMR parameters of the dominant P1′ Ala conformer show only subtle differences from those of the template peptide. An increased backbone amide proton temperature coefficient of the P1′ position (+2.2 versus −0.7 ppb/K) may indicate that the strength of the backbone hydrogen bond of this residue is modulated due to the loss of side-chain hydrogen bonding (Fig. 3). This contrasts with the backbone amide proton temperature coefficient of the P5′ position, which remains unchanged at −1.7 ppb/K. For this hydrogen-bond donor the corresponding acceptor can therefore be confirmed as the P2 Thr side-chain hydroxyl as previously suggested by geometric criteria [26] because the alternative P1′ side-chain acceptor has been disabled (Fig. 3). This substitution surprisingly affects the pattern of the NOE connectivities of only one residue within experimental error, namely that of P5′ Gln. An additional NOE is observed between the P5′ Gln backbone HN and the P1′ Hβ, which would be expected for a P1′ Ser → Ala substitution in the absence of any associated structural rearrangement. Four weak non-sequential NOEs from the Hβ of P5′ Gln are not observed in the spectra of the P1′ Ala variant. This is reflected in an increased level of disorder of this side chain in the families of calculated structures (Fig. 3). In order to test whether there is a communication between the P1′ and P5′ side chains, the P5′ Gln → Ala variant of the template was synthesised and analysed.

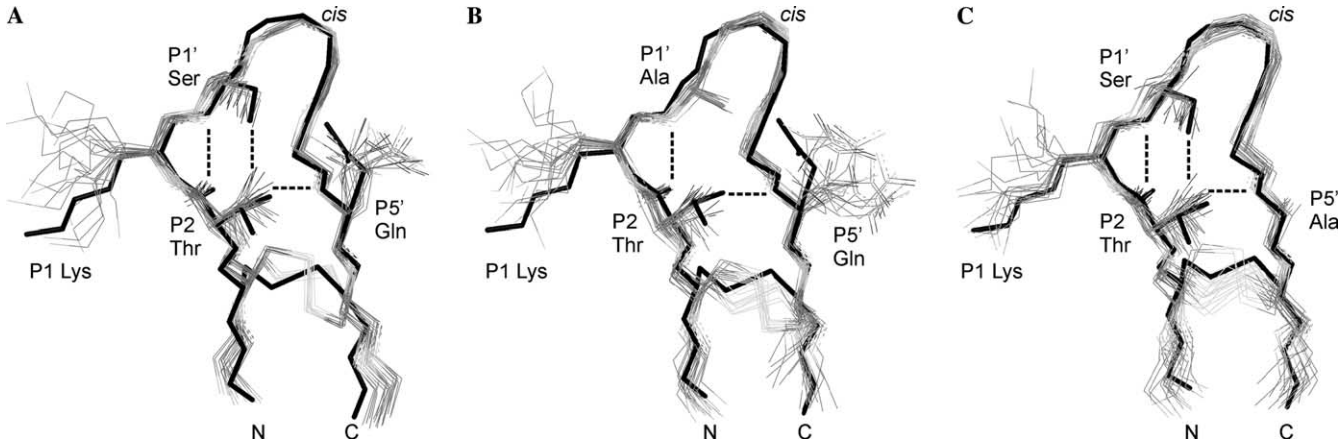

Fig. 3. Superimposition of the families of 20 lowest-energy distance geometry/simulated annealing structures calculated from NMR data (O, C, N, and S atoms are shown in increasingly lighter shades of grey) onto the X-ray crystal structure of the reactive site loop of mung bean BBI protein in complex with trypsin (black sticks; residues 17–27 [17]). Only selected side chains and potential hydrogen bonds (dashed lines) are shown for clarity. The *cis* peptide bond and the peptide termini are indicated. The pairwise r.m.s. deviations over the covalently closed backbone (P3 Cys to P6′ Cys) within the individual families of structures are 0.34 (±0.11) Å for the template peptide (A), 0.39 (±0.10) Å for the P1′ Ala variant (B), and 0.53 (±0.15) Å for the P5′ Ala variant (C). The r.m.s. deviations from the corresponding stretch of backbone of the protein crystal structure are 0.50 (±0.11) Å, 0.62 (±0.11) Å, and 0.54 (±0.12) Å, respectively.

Comparison with the effects of the P5′ Gln → Ala substitution

The biological activities of the P1′ Ala and P5′ Ala variant are indistinguishable within experimental error, with the exception of the inhibitory active fraction of the P5′ Ala variant, which is more similar to that of the template (Table 1) as confirmed by the NMR spectra (Fig. 2). The resonances of the two most highly populated conformers of the P5′ Ala variant could be fully assigned. $H\alpha_i$–$H\alpha_{i+1}$ NOE connectivities, which are diagnostic of *cis* peptide bonds [27], confirm that the conformational heterogeneity arises from *cis*/*trans* peptide bond isomerisation. While the dominant conformer retains the protein-like *cis* peptide bond at P3′ Pro, the *cis* peptide bond is shifted to the neighbouring P4′ Pro in the minor conformer. The protein-like structure of the dominant conformer is confirmed by the family of 20 lowest-energy distance geometry/simulated annealing structures (Fig. 3) compatible with the NMR-derived distance restraints (20 sequential (i, $i+1$), 2 medium range (i, $i+2$ to i, $i+3$), and 6 long range (i, $i+6$ to i, $i+8$)), and dihedral angle restraints (10ω, 10ϕ, 4χ^1). Comparing the NMR parameters (chemical shifts, amide proton temperature coefficients, and $^3J_{HNH\alpha}$ coupling constants) of the P1′ Ser in the template peptide and the P5′ Ala peptide, as well as the NMR parameters of the P5′ Gln residue in the template peptide and the P1′ Ala peptide, we did not find sufficient differences to confirm a fixating direct interaction such as a hydrogen bond between the side chains of the P1′ Ser and P5′ Gln residues in solution.

Conclusions

The "stubbornly" conserved P1′ Ser of BBI proteins is not essential for the structural integrity of the reactive site loop. The side-chain oxygen atom with its crystallographically confirmed intramolecular hydrogen bonding is structurally dispensable. Its loss, however, marginally weakens the trypsin affinity and the same reduced affinity is observed upon cropping the side chain of the P5′ residue to that of an Ala. These thermodynamic findings are reproduced by the analogous variants of an SFTI-1-derived proteinomimetic with a different natural P5 residue (Ile) [12]. The NMR data do not indicate a fixed interaction between the side chains of P1′ Ser and P5′ Gln in solution. Transient interactions, however, remain a possibility, in particular because these two side chains may approach each other within hydrogen-bond distance as observed in some BBI crystal structures [17,28,29] but not in others [16,20,30]. Less than half of the P1′ Ser side-chain surface is solvent accessible. This compact arrangement is partly the result of the BBI-typical main chain reversal by the *cis* peptide bond (Fig. 3) at the centre of a type VIb β-turn which is formed by the P1′ to P4′ residues. While a hydrogen bond across this turn between the P1′ Ser side chain and the backbone carbonyl of the P3′ residue is a possibility (not shown), its certain absence in the P1′ Ala variant is of little structural impact. We conclude that the general potential of P1′ substitutions for optimising inhibition and selectivity [31,32] in this system is best further explored in concert with the P5′ and P2 residues, for example, in a combinatorial format. The side chains of these three residues are located on the same face of the

β-hairpin and may interact or compete for the same space (Fig. 3). A particular interaction is the hydrogen bond between the side chains of P1′ Ser and P2 Thr because its length shortens from 3.2 Å in the unbound inhibitor [30] to 3.0 Å [33] or even 2.9 Å [2] in complex with trypsin while the distances of the other intramolecular hydrogen bonds shown in Fig. 3A remain unchanged. An analogous intramolecular hydrogen bond in turkey ovomucoid third domain that contracts upon complexation with chymotrypsin has been demonstrated to translate into a gain of binding free energy [34]. The loss of this energetic increment by a P1′ Ser → Ala substitution may contribute to the observed reduction in trypsin affinity. Such interactions and potential steric conflicts may help to explain why reported point mutations of the P1′ Ser in BBI proteins invariably weakened the inhibitory potency [35,36]. An intramolecular steric conflict was also identified as a reason for the preference of small P1′ residues in bovine pancreatic trypsin inhibitor [37]. The additional spatial freedom, in part provided by an extended backbone conformation, may help to explain the presence of larger amino acids at the P1′ locus in most other canonical serine proteinase inhibitor families [14].

Acknowledgments

The authors wish to thank S.J. Matthews, J.D. McBride, R. Cooke, H. Toms, P. Haycock, and J. Barton for helpful discussions and technical assistance. We thank W. Bode for the coordinates of mung bean BBI in complex with trypsin and gratefully acknowledge the financial support of GlaxoSmithKline.

References

[1] B. Prakash, S. Selvaraj, M.R. Murthy, Y.N. Sreerama, D.R. Rao, L.R. Gowda, Analysis of the amino acid sequences of plant Bowman–Birk inhibitors, J. Mol. Evol. 42 (1996) 560–569.
[2] S. Luckett, R.S. Garcia, J.J. Barker, A.V. Konarev, P.R. Shewry, A.R. Clarke, R.L. Brady, High-resolution structure of a potent, cyclic proteinase inhibitor from sunflower seeds, J. Mol. Biol. 290 (1999) 525–533.
[3] A.B.E. Brauer, G. Kelly, J.D. McBride, R.M. Cooke, S.J. Matthews, R.J. Leatherbarrow, The Bowman–Birk inhibitor reactive site loop sequence represents an independent structural β-hairpin motif, J. Mol. Biol. 306 (2001) 799–807.
[4] W. Bode, R. Huber, Natural protein proteinase-inhibitors and their interaction with proteinases, Eur. J. Biochem. 204 (1992) 433–451.
[5] J.D. McBride, E.M. Watson, A.B.E. Brauer, A.M. Jaulent, R.J. Leatherbarrow, Peptide mimics of the Bowman–Birk inhibitor reactive site loop, Biopolymers 66 (2002) 79–92.
[6] I. Schechter, A. Berger, On the size of the active site in proteases. I. Papain, Biochem. Biophys. Res. Commun. 27 (1967) 157–162.
[7] G.J. Domingo, R.J. Leatherbarrow, N. Freeman, S. Patel, M. Weir, Synthesis of a mixture of cyclic peptides based on the Bowman–Birk reactive site loop to screen for serine protease inhibitors, Int. J. Pept. Protein Res. 46 (1995) 79–87.
[8] J.D. McBride, A.B.E. Brauer, M. Nievo, R.J. Leatherbarrow, The role of threonine in the P2 position of Bowman–Birk proteinase inhibitors: studies on P2 variation in cyclic peptides encompassing the reactive site loop, J. Mol. Biol. 282 (1998) 447–457.
[9] A.B.E. Brauer, M. Nievo, J.D. McBride, R.J. Leatherbarrow, The structural basis of a conserved P2 threonine in canonical serine proteinase inhibitors, J. Biomol. Struct. Dyn. 20 (2003) 645–656.
[10] T. Gariani, J.D. McBride, R.J. Leatherbarrow, The role of the P2′ position of Bowman–Birk proteinase inhibitor in the inhibition of trypsin—studies on P2′ variation in cyclic peptides encompassing the reactive site loop, Biochim. Biophys. Acta 1431 (1999) 232–237.
[11] A.B.E. Brauer, G.J. Domingo, R.M. Cooke, S.J. Matthews, R.J. Leatherbarrow, A conserved *cis* peptide bond is necessary for the activity of Bowman–Birk inhibitor protein, Biochemistry 41 (2002) 10608–10615.
[12] A. Descours, K. Moehle, A. Renard, J.A. Robinson, A new family of β-hairpin mimetics based on a trypsin inhibitor from sunflower seeds, ChemBioChem 3 (2002) 318–323.
[13] M. Laskowski Jr., I. Kato, Protein inhibitors of proteinases, Annu. Rev. Biochem. 49 (1980) 593–626.
[14] W. Apostoluk, J. Otlewski, Variability of the canonical loop conformations in serine proteinases inhibitors and other proteins, Proteins Struct. Func. Genet. 32 (1998) 459–474.
[15] Y. Tsunogae, I. Tanaka, T. Yamane, J. Kikkawa, T. Ashida, C. Ishikawa, K. Watanabe, S. Nakamura, K. Takahashi, Structure of the trypsin-binding domain of Bowman–Birk type protease inhibitor and its interaction with trypsin, J. Biochem. 100 (1986) 1637–1646.
[16] P. Chen, J. Rose, R. Love, C.H. Wei, B.C. Wang, Reactive sites of an anticarcinogenic Bowman–Birk proteinase-inhibitor are similar to other trypsin-inhibitors, J. Biol. Chem. 267 (1992) 1990–1994.
[17] G.D. Lin, W. Bode, R. Huber, C.W. Chi, R.A. Engh, The 0.25 nm X-ray structure of the Bowman–Birk-type inhibitor from mung bean in ternary complex with porcine trypsin, Eur. J. Biochem. 212 (1993) 549–555.
[18] I.L. de la Sierra, L. Quillien, P. Flecker, J. Gueguen, S. Brunie, Dimeric crystal structure of a Bowman–Birk protease inhibitor from pea seeds, J. Mol. Biol. 285 (1999) 1195–1207.
[19] H.K. Song, Y.S. Kim, J.K. Yang, J. Moon, J.Y. Lee, S.W. Suh, Crystal structure of a 16 kDa double-headed Bowman–Birk trypsin inhibitor from barley seeds at 1.9 Å resolution, J. Mol. Biol. 293 (1999) 1133–1144.
[20] J. Koepke, U. Ermler, E. Warkentin, G. Wenzl, P. Flecker, Crystal structure of cancer chemopreventive Bowman–Birk inhibitor in ternary complex with bovine trypsin at 2.3 Å resolution. Structural basis of Janus-faced serine protease inhibitor specificity, J. Mol. Biol. 298 (2000) 477–491.
[21] H. Nakata, S. Ishii, Substrate activation of trypsin and acyltrypsin caused by α-*N*-benzoyl-L-arginine *p*-nitroanilide, J. Biochem. 72 (1972) 281–290.
[22] H. Edelhoch, Spectroscopic determination of tryptophan and tyrosine in proteins, Biochemistry 6 (1967) 1948–1954.
[23] M.E. Hodsdon, J.W. Ponder, D.P. Cistola, The NMR solution structure of intestinal fatty acid-binding protein complexed with palmitate: application of a novel distance geometry algorithm, J. Mol. Biol. 264 (1996) 585–602.
[24] G. Wagner, W. Braun, T.F. Havel, T. Schaumann, N. Go, K. Wüthrich, Protein structures in solution by nuclear magnetic resonance and distance geometry. The polypeptide fold of the basic pancreatic trypsin-inhibitor determined using 2 different algorithms, DISGEO and DISMAN, J. Mol. Biol. 196 (1987) 611–639.
[25] R.A. Laskowski, M.W. Macarthur, D.S. Moss, J.M. Thornton, PROCHECK—a program to check the stereochemical quality of protein structures, J. Appl. Cryst. 26 (1993) 283–291.

[26] A.B.E. Brauer, G. Kelly, S.J. Matthews, R.J. Leatherbarrow, The ^{1}H-NMR solution structure of the antitryptic core peptide of Bowman–Birk inhibitor proteins: a minimal canonical loop, J. Biomol. Struct. Dyn. 20 (2002) 59–70.

[27] K. Wüthrich, NMR of Proteins and Nucleic Acids, Wiley, New York, 1986.

[28] Y.L. Li, Q.C. Huang, S.W. Zhang, S.P. Liu, C.W. Chi, Y.Q. Tang, Studies on an artificial trypsin-inhibitor peptide derived from the mung bean trypsin-inhibitor—chemical synthesis, refolding, and crystallographic analysis of its complex with trypsin, J. Biochem. 116 (1994) 18–25.

[29] R.H. Voss, U. Ermler, L.O. Essen, G. Wenzl, Y.M. Kim, P. Flecker, Crystal structure of the bifunctional soybean Bowman–Birk inhibitor at 0.28 nm resolution—structural peculiarities in a folded protein conformation, Eur. J. Biochem. 242 (1996) 122–131.

[30] J.E. Debreczeni, G. Bunkoczi, B. Girmann, G.M. Sheldrick, In-house phase determination of the lima bean trypsin inhibitor: a low-resolution sulfur-SAD case, Acta Crystallogr. D 59 (2003) 393–395.

[31] S. Grahn, T. Kurth, D. Ullmann, H.D. Jakubke, S′ subsite mapping of serine proteases based on fluorescence resonance energy transfer, Biochim. Biophys. Acta 1431 (1999) 329–337.

[32] Z. Malik, S. Amir, G. Pal, Z. Buzas, E. Varallyay, J. Antal, Z. Szilagyi, K. Vekey, B. Asboth, A. Patthy, L. Graf, Proteinase inhibitors from desert locust, *Schistocerca gregaria*: engineering of both P-1 and P-1′ residues converts a potent chymotrypsin inhibitor to a potent trypsin, Biochim. Biophys. Acta 1434 (1999) 143–150.

[33] Y.S. Zhu, Q.C. Huang, C.W. Chi, Crystal structure of mung bean inhibitor lysine active fragment complex with bovine β-trypsin at 1.8 Å resolution, J. Biomol. Struct. Dyn. 16 (1999) 1219–1224.

[34] M. Laskowski, M.A. Qasim, Z.P. Yi, Additivity-based prediction of equilibrium constants for some protein–protein associations, Curr. Opin. Struct. Biol. 13 (2003) 130–139.

[35] S. Odani, T. Ikenaka, Studies on soybean trypsin inhibitors. XIV. Change of the inhibitory activity of Bowman–Birk inhibitor upon replacements of the α-chymotrypsin reactive site serine residue by other amino acids, J. Biochem. 84 (1978) 1–9.

[36] T. Kurokawa, S. Hara, T. Teshima, T. Ikenaka, Chemical replacement of P1′ serine residue in the second reactive site of soybean protease inhibitor C-II, J. Biochem. 102 (1987) 621–626.

[37] A. Grzesiak, R. Helland, A.O. Smalas, D. Krowarsch, M. Dadlez, J. Otlewski, Substitutions at the P1′ position in BPTI strongly affect the association energy with serine proteinases, J. Mol. Biol. 301 (2000) 205–217.